Escola de Primavera de Transição e Turbulência
Blumenau 2022

ABCM Associação Brasileira de Engenharia e Ciências Mecânicas

13th Spring School on Transition and Turbulence
September 19th-23rd, 2022, Blumenau, SC, Brazil

EPTT-2022-0070
ASSESSING THE SIZE AND POSITION OF PARTICLE CLUSTERS IN THE GAS-SOLID FLOW OF A CFB RISER USING HIGH-SPEED IMAGING AND IMAGE ANALYSIS

Vivien Rossbach
State University of Campinas – Campinas, Brazil
University of Blumenau – Blumenau, Brazil
vrossbach@furb.br

Sarah L. Becker
Federal University of Santa Catarina – Florianopolis, Brazil
sarahlaisa@gmail.com

Vinicius Vale
Denise Bahr
Henry F. Meier
University of Blumenau – Blumenau, Brazil
vinivale@gmail.com
deniseeq@gmail.com
meier@furb.br

Dirceu Noriler
State University of Campinas – Campinas, Brazil
dnoriler@unicamp.br

Abstract. *In turbulent gas-solid systems, the development of clusters of solid particles reduces the efficiency of the gas-solid contact, as the clusters have a larger size and a smaller void fraction than the individual dispersed particles. Experimental measurement of cluster size is very difficult because of the fast changes in the flow velocity and concentration. However, the size of a cluster can be estimated through high-quality images taken at minor intervals or through numerical simulations, according to the literature. This study aims to estimate, from high-speed imaging, the size and position of the particle clusters in the gas-solid flow of a pilot-scale CFB riser. Through images with high resolution obtained during 8 s, the size and average position of particle clusters in the inlet region of the riser were estimated under different operating conditions.*

Keywords: *Gas-solid flow, High-Speed Imaging, CFB riser.*

1. INTRODUCTION

The fluidization of solid particles is an important process used in several industrial applications, mainly in fluidized beds. In the circulating fluidized bed (CFB), particles are continuously fed into a riser and carried by an upward flow of gas. Operations in CFB risers might face difficulties because of the formation of clusters. They are regions concentrated in particles due to hydrodynamics effects and weak interparticle forces. These clusters are formed by inelastic collisions between particles, which dissipate kinetic energy and reduce particle velocity and gas pressure due to viscous dissipation (Wang et al., 2009). Then the gas and the neighboring particles flow toward these low-pressure regions, forming clusters. Energy dissipation in dilute and turbulent beds, such as those found in CFB risers, is mainly due to hydrodynamic instabilities. As the energy dissipation of inelastic collisions reduces the distance of particles, forces between particles increase and become relevant concerning the hydrodynamic instabilities (Cahyadi et al., 2017).

The formation of clusters influences flow parameters such as particle slip velocity, drag force, pressure drop, local void fraction, mixing, and heat and mass transfer. It impairs the efficiency of the gas-solid contact, reducing the yield of reactions and affecting processes of interest that depend on this contact (Namkung and Kim, 1998). These structures are studied by a large group of authors in the literature to reduce their formation. The characterization of clusters in experimental efforts is made by distinct methods, categorized as invasive or non-invasive and optical or non-optical. The non-invasive techniques have advantages because they do not disturb the hydrodynamics of the flow analyzed. However, difficulties with data interpretation are common in these methods. Optical techniques can obtain information

about particle behavior. They are based on the absorption or transmittance of light or infrared wavelengths in the electromagnetic spectrum. While non-optical methods are based on acoustic or electrical probe signals. The acquisition of experimental parameters such as cluster diameter is very complex. These structures are irregular and present rapid variations in velocity and concentration, common in two-phase flow. The cluster diameter can be estimated by images of the flow, taken within a short time interval, and also by numerical simulations (Cahyadi et al., 2017).

High-speed imaging is an alternative to enable the study of the real-time behavior of gas-solid flow in CFB risers by Digital Image Analysis (DIA). Link et al. (2005) was the first study to extract full-field experimental data of solids mass flux by combining particle image velocimetry (PIV) with DIA to determine solids volume fraction. Later, Laverman et al. (2008) applied local image filters to improve the quality of the images. These were converted into porosity fields by a linear correlation. Van Buijtenen et al. (2010) linked solids volume fraction to normalized intensity data. In this regard, the authors used a two-parameter equation calibrated with the weight of the solid in the fluidized bed. Images from simulations were used to find parameters for the correlation. De Jong et al. (2012) verified that the correlation between solids volume fraction and light intensity has fixed parameters for a given fluidization condition.

Varas et al. (2016) introduce a DIA post-processing method based on a temporal histogram algorithm. It provides reliable solid volume fraction data, removing image imperfections and only accounting for the particles' intensity. CFD-DEM simulations were related to the camera images, looking for the correspondence between them. So it was possible to differentiate what is noise and shadow. A contribution of this technique is the implementation of subpixel intensity, to achieve similarity with the experimental images. Thus, it was possible to obtain data from experiments with non-ideal and inhomogeneous illumination, which are not sensitive to lighting conditions. Moreover, the authors employed a temporal filter that provides intensity data that is directly proportional to the pixels covered by the solid phase.

This study aims to investigate the size and position of particle clusters with high-speed imaging in a pilot-scale CFB riser. High-resolution images of gas-solid flow were obtained during 8 s to estimate the size and average position in the inlet region of the riser under different operating conditions. The results were post-processed with ImageJ and an in-house Python code, enabling us to estimate solids volume fraction, and also the position and size of the particle clusters.

2. MATERIAL AND METHODS

The experimental data used in this study were gathered in a pilot-scale CFB unit located in the Laboratory of Verification and Validation (LVV), at the University of Blumenau. The pilot-scale CFB riser, illustrated in Fig. 1-a, has 15.5 m of height and an inner diameter of 0.1 m. The solids inlet is an adjacent pipe with a 45° of an inclination concerning the vertical riser, and the outlet also has an inclination of 10° regarding the solids inlet. Gas-solid flow in the riser comprises a gas phase represented by air at ambient conditions, and a solid phase represented by FCC particles with a density of 1450 kg/m³ and a mean Sauter diameter of 67 μm. Therefore, the experiments were made under two experimental conditions. The first condition has a gas superficial velocity of 10 m/s and a solids mass flux of 1.13 kg/m²s, and the second one has a gas superficial velocity of 10 m/s and a solids mass flux of 4.21 kg/m²s.

The experimental setup was mounted in the three height positions of the riser and the camera was positioned to focus on a plane located in the center of the riser. To ensure that this plane has been focused, we positioned a ruler in the lateral of the riser, aligned with its center line. In the calibration step, the light reflector was positioned in front of the riser to allow us a view of the ruler marking. The camera focus was adjusted to improve the visualization of the rule marking. The images taken with the rule in this position were used to quantify how many pixels correspond to a known distance shown in the rule. This procedure was adopted to calibrate the digital image analysis algorithm. The calibrations found for the measurements done at 1 m, 5.5 m, and 10.1 m height were 13.6401 pixels/mm, 15.0802 pixels/mm, and 13.2222 pixels/mm, respectively. These calibrations correspond to an average of 65 μm/pixel, which is closer to the mean particle diameter. Thus, our method is not capable of detecting a single particle, because it is necessary to have at least 2 pixels in one particle to determine its diameter. For this reason, this method can detect only clusters of particles and estimate their size and position.

For each operating condition and the three axial positions defined, 1000 images were acquired with a frequency of 125 Hz, using an IDT 053-V3-S1 camera and a LED reflector with a power of 50 W and a light temperature of 5500 K. The LED reflector was positioned behind the CFD riser, as shown in Fig. 1, and the camera was positioned in front of this one, with a focal distance of 41 cm from the riser center.

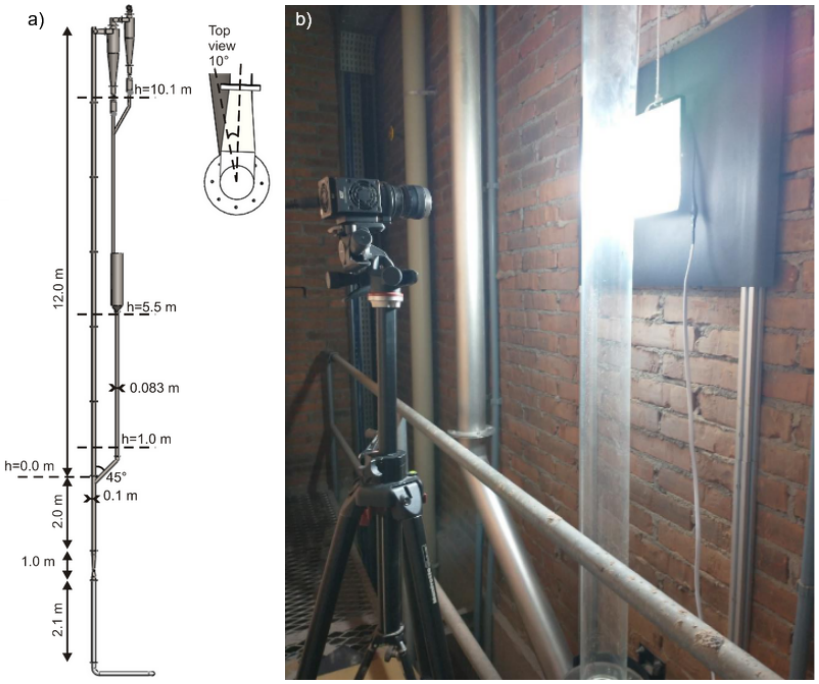

Figure 1 - Dimensions of the pilot-scale CFB unit (a), and photo of the experimental setup (b).

Figure 2 shows an algorithm with the steps kept to perform the data acquisition with the high-speed camera and the digital image analysis using ImageJ and Python. The solid particle diameter calculated by the Python code was validated using 2 images, where a circle with 2 cm of diameter is positioned in different places. The image scale was set in ImageJ by drawing a line corresponding to the circle diameter. This step resulted in a scale of 4.68 pixels/mm. The results of the particle analysis were given by ImageJ in pixels and exported to be used in the Python code, where the diameter calculation using the calibration and the particle size in pixels resulted in a mean diameter of 19.97 mm for the two circles.

For each test, the initial step is the global calibration. A single image with a ruler focused in the riser center was used for this calibration, as discussed earlier in this session. The resulting scale is set as global and the 1000 images are uploaded as an image sequence in ImageJ. All the images are cropped in a window of 50 mm in length and 60 mm in height. The cropped images are sharpened to increase the contrast between the particles and the background. The next step is to remove the white background by specifying an intensity equal to 255. The particle analyzer macro is applied to the image group and detects particles larger than 50 pixels. However, to analyze all the particles captured in the images, we changed the minimum particle diameter from 50 pixels to 0 pixels and the maximum particle diameter to infinity, as we intend to detect clusters. The particle analysis results in a .csv file that is exported to be used as a dataset in the Python code.

The analysis steps in Python consist of data wrangling, exploratory and statistical analysis, and visual analysis of the results. The .csv files obtained in ImageJ were imported into a Jupyter notebook, where the calibration results were used to remove particles with a diameter smaller than 2 pixels. To calculate the solid volume fraction in each axial position, we used the 50 mm x 60 mm frames. The volume of the particles detected in the frame was calculated assuming spherical particles, then the results were corrected using the circularity obtained from ImageJ. The particle volume summation was divided by the volume of the corresponding riser section, with a height of 60 mm and a diameter of 50 mm, to obtain the solid volume fraction, according to Equation 1.

$$f_s = \frac{1}{\pi D_{riser}{}^2/4} \cdot \sum_{i=1}^{1000} \left(\frac{\pi d_p{}^2}{4 \cdot circularity} \right) \quad (1)$$

Contours of solid volume fractions were calculated for each frame using pivot tables where the solid volume fractions were aggregated in the axial and radial positions using its mean value. The solids dispersion coefficient (CV) proposed by Rossbach et al. (2019) was used to evaluate the particle distribution in the frames. This is a statistical coefficient calculated as the ratio between the standard deviation and the mean solid volume fraction, as shown in Equation 2, where n is the number of particles detected in each frame. Lower dispersion coefficients indicate more

homogeneous solids dispersions and values of Cv smaller than 1.0 are desirable for a good solids dispersion in the CFB riser.

$$C_V = \frac{1}{\bar{f}_s} \cdot \sqrt{\frac{\sum_{i=1}^{n} (f_{s,i} - \bar{f}_s)^2}{n-1}} \tag{2}$$

The mean particle diameter was calculated by Equation 3, using the particle area, which was calculated in ImageJ using the respective frame calibration, given in µm/pixel.

$$d_p(\mu m) = \frac{1\ mm}{1000\ \mu m} \cdot \sqrt{\frac{A\ (mm^2) \cdot 4}{\pi}} \tag{3}$$

The non-supervised machine learning algorithm K-Means (Na et al., 2010) was used to divide particles into 7 groups according to their diameter.

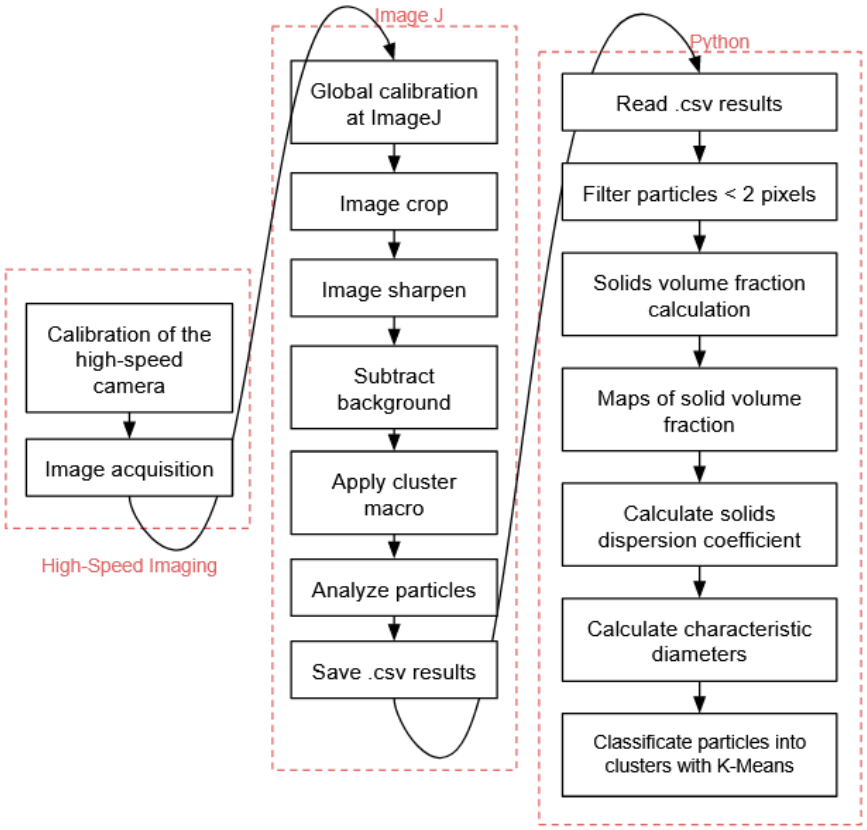

Figure 2 - Sequential steps for the experimental procedure and the digital image analysis.

Figure 3 shows the results obtained in each step of the image processing in ImageJ. All the steps were applied to the batches with 1000 bitmap images. The first frame shows the original image captured on the riser's left side, including the wall and the bottom label that indicates the axial position. The second frame shows the 50 mm x 60 mm cropped area obtained from the original image, which corresponds to half of the riser diameter. The image in the third frame was sharpened to highlight the contour of the particles and to distinguish them from the background. In the fourth frame, the background corresponding to a color intensity equal to 255 was removed and the resulting image is expected to have only particles with intensity values measured on a grayscale. The Particle Cluster Analyzer macro from ImageJ was used to detect particle clusters and calculate their areas, as shown in the fifth frame. The results including particle area and circularity were obtained in a .csv format from the highlighted particles in the last frame.

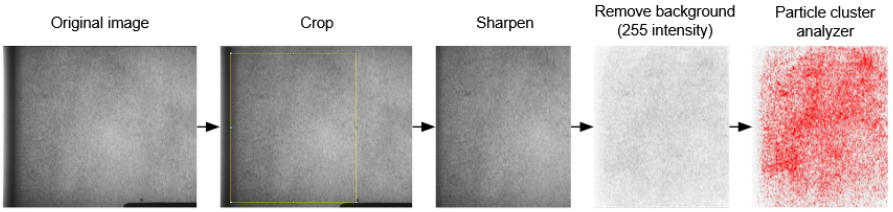

Figure 3 - Illustration of the steps for image pre-processing with ImageJ.

3. RESULTS AND DISCUSSION

Figure 4 shows the solid volume fraction contours calculated for the CFB riser in three axial positions and 2 operating conditions. These contours show the solid volume fraction calculated for particles focused in the center plane of the riser, at the center radial position of the riser illustrated on the left side of Figure 4. A global analysis indicates that, in both operating conditions, the solids particles are more concentrated near the solids inlet, at the axial position of 1.0 m. In contrast, solids concentration is lower at a height of 10.1 m. The solid volume fraction contours have missing areas due to defects in the riser acrylic wall, which were removed by normalizing the data. At 1.0 m height, solid particles are more concentrated in the left wall, which is opposite the solids inlet. The same trend was observed for both operating conditions, but the solids concentration is higher along the radial direction for a solids flux of 4.21 kg/m²s. A greater solid volume fraction was observed for the most diluted condition, with solids flux equal to 1.13 kg/m²s, at 5.5 m and 10.1 m height. The solid volume fraction in these positions is larger than 0.001 for the solids flux of 1.13 kg/m²s and between 0.0001 and 0.001 for the solids flux of 4.21 kg/m²s.

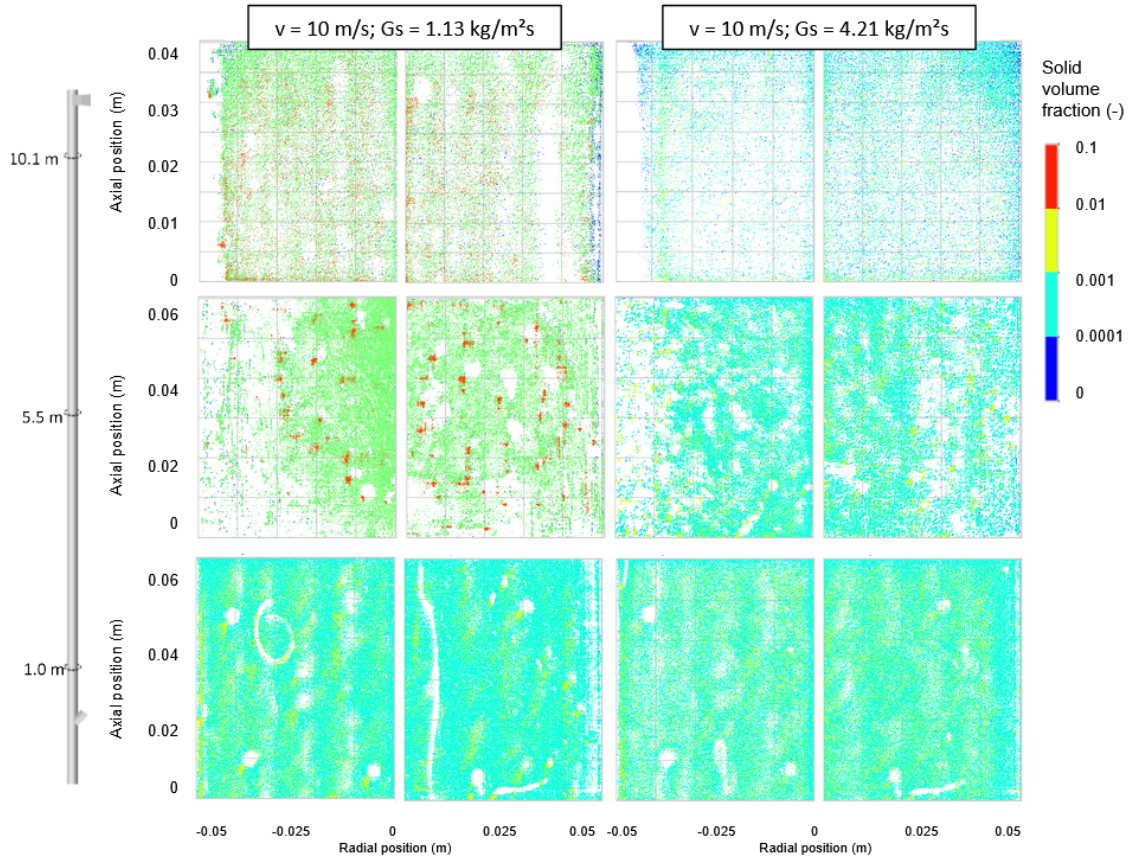

Figure 4 - Contours of solid volume fraction distributions for the experiments with v = 10 m/s and G_s = 1.13 kg/m²s, v = 10 m/s and G_s = 4.21 kg/m²s at the three measurement heights.

The results obtained for the solids flux of 4.21 kg/m²s are typical for CFB risers under these operating conditions, as shown by Rossbach et al. (2019). These results need more investigation to determine whether the result was influenced by particle concentration. One hypothesis to be studied is that the result obtained for the solids flux of 1.13 kg/m²s is more accurate, as the technique used is appropriate for dilute beds. In this way, it is easier for the camera to detect particles in the center plane of the riser under very dilute conditions. With a solids flux of 4.21 kg/m²s, which is more concentrated, particles flowing near the wall may obstruct the detection of particles in the central plane.

Table 1 shows the number of particles classified into 7 clusters, numbered from 0 to 6, for the operating condition with v = 10 m/s and Gs = 1.13 kg/m²s. On the riser left side, at 1 m heigh there are 19676 particles grouped into cluster 5, and their mean diameter is 618 μm. Cluster 0 has 31 particles, or clusters, with a mean diameter of 15,169 μm. The maximum cluster size detected is 53,590 μm and there are 6 clusters of particles whose mean diameter is higher than 40,000 μm. On the right side, cluster 0 has 29169 particles with a mean diameter of 712 μm and clusters with a mean diameter lower than those detected on the left side, which is opposite to the solids inlet and parallel to the riser outlet. At 5.5 m high, the number of particles detected and their mean diameter is similar to the results found at 1 m high. Most particles were detected at 1 m and 5.5 m height, and fewer particles were detected at 10.1 m. Also, the clusters' mean diameter is lower at 10.1 m than in the other axial positions. These results suggest that solid particles are more concentrated in the lower axial positions due to the pressure drop and back mixing, increasing the solids inventory and the residence time.

Table 1 - Particles in each diameter class for the left and the right side of the riser for v = 10 m/s and G_s = 1.13 kg/m²s.

Side	**Cluster**	**h = 1.0 m**		**h = 5.5 m**		**h = 10.1 m**	
		Diameter (μm)	**Counts**	**Diameter (μm)**	**Counts**	**Diameter (μm)**	**Counts**
Left side	0	15,169	31	712	25255	368	338
	1	41,426	4	22,329	2	3,630	6
	2	53,590	1	26,938	2	2,195	10
	3	37,257	3	17,096	2	3,557	5
	4	23,265	6	11,414	8	1,263	8
	5	618	19676	20,755	1	984	23
	6	47,021	1	6,959	41	704	53
Right side	0	712	29169	368	338	425	139
	1	28,874	2	3,630	6	7,304	3
	2	33,554	2	2,195	10	7,007	1
	3	23,782	2	3,557	5	7,405	1
	4	16,020	6	1,263	8	7,247	2
	5	9,932	22	984	23	7,345	2
	6	27,376	1	704	53	2,493	1

Table 2 shows the number of particles classified into clusters numbered from 0 to 6, under the operating condition with v = 10 m/s and Gs = 4.21 kg/m²s. Most of the particles have a mean diameter between 586 μm and 786 μm. The mean diameter of this major class decreases within the riser height, which indicates that small particles are carried by the flow, while larger particles have a greater residence time inside the riser. Clusters with a diameter higher than 100,000 μm were found, particularly at 5.5 m high. We can observe that, with an increase in the solid mass flux, clusters with a larger diameter are found in the intermediate region of the riser. When the solid mass flux decreases, however, larger clusters are found near the solids inlet. Particle clusters with a diameter larger than 100,000 μm were detected on the left side of the riser, while the clusters found on the right side have a size similar to that found with Gs = 1.13 kg/m²s. However, on the right side, the clusters detected at 10.1 m heigh are larger than on the left side, because on the right side there is a back mixing of particles coming from the gas and solids outlet.

Table 2 - Particles in each diameter class for the left and the right side of the riser for v = 10 m/s and G_s = 4.21 kg/m²s.

Side	Cluster	h = 1.0 m		h = 5.5 m		h = 10.1 m	
		Diameter (µm)	Counts	Diameter (µm)	Counts	Diameter (µm)	Counts
Left side	0	786	21922	668	22440	586	18273
	1	112,016	3	134,816	3	77,376	4
	2	81,062	2	125,095	2	88,369	1
	3	117,381	2	114,280	1	48,872	3
	4	103,441	2	127,883	2	72,866	3
	5	70,128	2	132,865	2	82,941	1
	6	48,275	2	136,158	2	27,020	11
Right side	0	750	23427	656	30853	589	6186
	1	63,117	2	82,022	3	76,086	2
	2	49,183	1	61,081	2	62,343	2
	3	72,563	2	74,551	2	45,660	3
	4	27,469	4	88,552	2	36,626	8
	5	60,042	1	41,831	2	51,629	3
	6	52,998	1	54,341	2	67,567	1

Figure 5 shows the solids dispersion coefficients of the solid volume fraction in the left and side half parts of the riser, at the three axial positions measured. At the most diluted operating condition, with v = 10 m/s and Gs = 1.13 kg/m²s, the solids dispersion coefficient near the solids inlet (h = 1.0 m) is higher on the left side than on the right side because the solids concentration near the wall that is the effect of the solids inlet. At the higher positions, however, solids concentration is higher on the right side of the riser, which can be an effect of the S-shape axial profile of solids concentration cited in the literature (Cahyadi et al., 2017).

With the more concentrated operating condition (v = 10 m/s, Gs = 4.21 kg/m²s), the solids dispersion coefficient has values higher than in the most dilute operating condition, and these values are higher on the left side than on the right side of the riser. This trend is observed at the three axial positions, different from what was observed in the most diluted operating condition. However, the solids dispersion with Gs = 4.21 kg/m²s is more equilibrated between the two half frames, with similar dispersion coefficients, as seen in Figure 5. In the comparison of the solids dispersion coefficients with the cluster results, we can see that, with a more concentrated gas-solid flow, greater clusters were detected, but the solids dispersion was more homogeneous along the radial position at the measurement points.

4. CONCLUSIONS

This study proposed a way to use the high-speed imaging technique to estimate cluster size and volume fraction in a CFB riser with a dilute flow and under turbulent conditions. ImageJ framework and a house-made Python code were used to post-process the high-resolution images obtained from the gas-solid flow in the CFB riser. This technique has some limitations, for example, the inability in dealing with dense flows, in which the central plane cannot be detected because of the interference of the particles flowing near the front wall. However, it was possible to trace solid volume fraction colormaps in which the estimated solid volume fraction range is similar to that observed in previous studies with similar operating conditions. Also, the solids dispersion coefficients measured are similar to that measured in previous studies. The K-Means model employed in our analysis enabled us to estimate the size of cluster particles and how they are distributed along the radial and axial positions of the CFB riser.

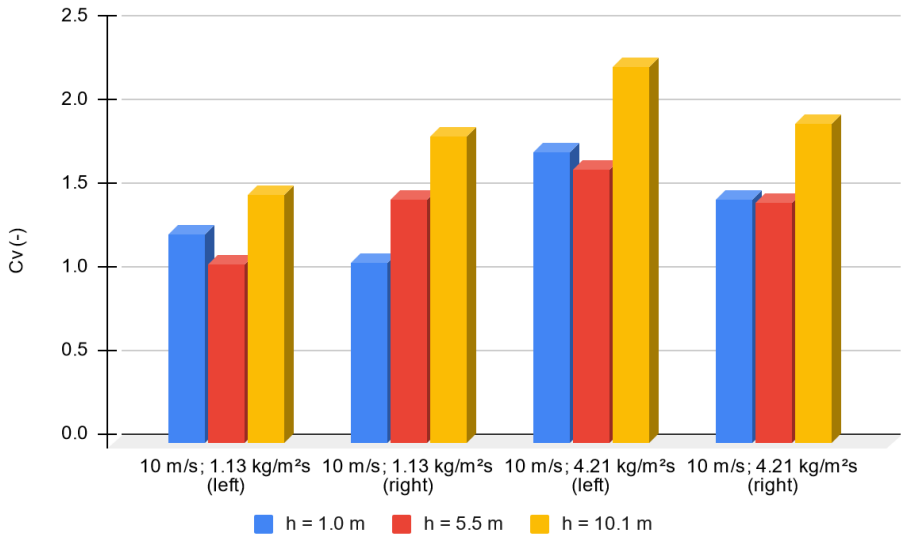

Figure 5 - Solids dispersion coefficient (C_v) for v = 10 m/s and G_s = 1.13 kg/m²s, and for v = 10 m/s and G_s = 4.21 kg/m²s, measured at three axial positions.

5. ACKNOWLEDGEMENTS

The authors are grateful for the financial support from the Human Resources Program of the National Agency for Petroleum, Natural Gas and Biofuels – PRH-ANP, supported with resources from the investment of oil companies qualified in the P, D&I Clause of ANP Resolution 50/2015, through the process Nº043919.

6. REFERENCES

Cahyadi, A., Anantharaman, A., Yang, S., Karri, S.B.R., Findlay, J.G., Cocco, R.A., and Chew, J.W., 2017. “Review of cluster characteristics in circulating fluidized bed (CFB) risers”. *Chemical Engineering Science*, Vol. 158, p. 70-95.

De Jong, J.F., Odu, S.O., Van Buijtenen, M.S., Deen, N.G., Van Sint Annaland, M., and Kuipers, J.A.M., 2012. “Development and validation of a novel digital image analysis method for fluidized bed particle image velocimetry”. *Powder Technology*. Vol. 230, p. 193-202.

Laverman, J.A., Roghair, I., Van Sint Annaland, M., and Kuipers, J.A.M., 2008. “Investigation into the hydrodynamics of gas–solid fluidized beds using particle image velocimetry coupled with digital image analysis”. *The Canadian Journal of Chemical Engineering*, Vol. 86, p. 523-535.

Link, J.M., Cuypers, L.A., Deen, N.G., and Kuipers, J.A.M., 2005. “Flow regimes in a spout–fluid bed: a combined experimental and simulation study”. *Chemical Engineering Science*, Vol. 60, p. 3425-3442.

S. Na, L. Xumin and G. Yong, 2010. "Research on k-means Clustering Algorithm: An Improved k-means Clustering Algorithm". *Third International Symposium on Intelligent Information Technology and Security Informatics*, p. 63-67.

Namkung, W. and Kim, S.D., 1998. “Gas backmixing in a circulating fluidized bed”. *Powder Technology*, Vol. 99, p. 70-78.

Van Buijtenen, M.S., Börner, M., Deen, N.G., Heinrich, S., Antonyuk, S., and Kuipers, J.A.M., 2011. “An experimental study of the effect of collision properties on spout fluidized bed dynamics”. *Powder Technology*, Vol. 206, p. 139-148.

Varas, A.E.C., Peters, E.A.J.F., Deen, N.G., and Kuipers, J.A.M., 2016. “Solids volume fraction measurements on riser flow using a temporal-histogram based DIA method”. *Aiche Journal*, Vol. 62, p. 2681-2698.

Wang, S., Li, X., Lu, H., Yu, L., Ding, J., and Yang, Z., 2009. “DSMC prediction of granular temperatures of clusters and dispersed particles in a riser”. *Powder Technology*, Vol. 192, p. 225-233.

7. RESPONSIBILITY NOTICE

The authors are the only ones responsible for the printed material included in this paper.